

# Interaction Effects Between Aquifer Thermal Energy Storage Systems

by Rogier Duijff<sup>1,2</sup>, Martin Bloemendal<sup>1,3,4</sup> , and Mark Bakker<sup>1</sup>

## Abstract

Aquifer thermal energy storage (ATES) is an energy efficient technique to provide heating and cooling to buildings by storage of warm and cold water in aquifers. In regions with large demand for ATES, ATES adoption has led to congestion problems in aquifers. The recovery of thermal energy stored in aquifers can be increased by reducing the distance between wells of the same temperature while safeguarding individual system performance. Although this approach is implemented in practice, the understanding of how this affects both the recovery efficiency and the needed pumping energy is lacking. In this research, the effect of well placement on the performance of individual systems is quantified, and guidelines for planning and design are developed. Results show an increase in thermal recovery efficiency of individual systems when the thermal zones of wells of the same temperature are combined, which is explained by reduced surface area of the thermal zone over which losses occur. The highest increase of the thermal recovery efficiency is found for systems with a small storage volume and long well screens. The relative increase of the thermal recovery efficiency is 12% for average-sized systems with a storage volume of 250,000 m<sup>3</sup>/year, and 25% for small systems (50,000 m<sup>3</sup>/year). The optimal distance between wells of the same temperature is 0.5 times the thermal radius, following the trade-off between an increase of the thermal recovery efficiency and the increase in pumping energy. The distance between wells of opposite temperature must be larger than three times the thermal radius to avoid negative interaction.

## Introduction

Around 40% of the worldwide energy demand is used for heating and cooling (REN21 2017). Aquifer thermal energy storage (ATES) is an efficient alternative to provide heating and cooling to buildings, with worldwide potential in regions with a temperate climate and suitable geology (e.g., Bloemendal et al. 2015). ATES systems consist of two wells: a warm well and a cold well (Figure 1). Cold

water is extracted from the aquifer by the cold well in the summer and is used directly for cooling. The water is heated up in the process and is injected back in the aquifer in the warm well, where it is stored until next winter. The flow is reversed in the winter when warm water is extracted from the warm well and used for heating, in combination with a heat pump to meet the required temperature. The water is cooled in the process and injected back in the aquifer by the cold well, completing the 1 year cycle. In temperate climates, the temperature of warm water injected by the warm well is 15 to 18 °C, while the temperature of the cold water injected by the cold well is 5 to 10 °C. ATES systems are energy efficient: 1 J of electric energy is needed to provide 20 to 40 J of thermal energy for cooling (e.g., Gao et al. 2017). This ratio is also called the Coefficient of Performance or COP. In the case of heating, 3 to 5 J of thermal energy is provided per Joule of electric energy (COP between 3 and 5). This COP is lower because the heat pump requires additional electric energy.

ATES is an increasingly popular technique to supply thermal energy to buildings, with wide application for utility buildings. ATES is especially popular in the Netherlands, where the large number of systems (>3000) and limited available aquifer volume has led to congestion problems in many urban areas (e.g., Bloemendal et al. 2018). The congestion problem is aggravated by inadequate design and planning. Current guidelines

<sup>1</sup>Water Management Department, Delft University of Technology, Delft, The Netherlands

<sup>2</sup>Energy Department, DWA, Gouda, The Netherlands

<sup>3</sup>Geohydrology Department, KWR Water Research Institute, Nieuwegein, The Netherlands

<sup>4</sup>Corresponding author: Water Management Department, Delft University of Technology, Delft, The Netherlands; j.m.bloemendal@tudelft.nl

*Article impact statement:* In this article, the effect of well placement on the recovery efficiency as well as on the required pumping energy of individual ATES systems is assessed and quantified. These results are used to develop guidelines for planning of ATES wells.

Received June 2021, accepted December 2021.

© 2021 The Authors. *Groundwater* published by Wiley Periodicals LLC on behalf of National Ground Water Association.

This is an open access article under the terms of the Creative Commons Attribution-NonCommercial-NoDerivs License, which permits use and distribution in any medium, provided the original work is properly cited, the use is non-commercial and no modifications or adaptations are made.

doi: 10.1111/gwat.13163

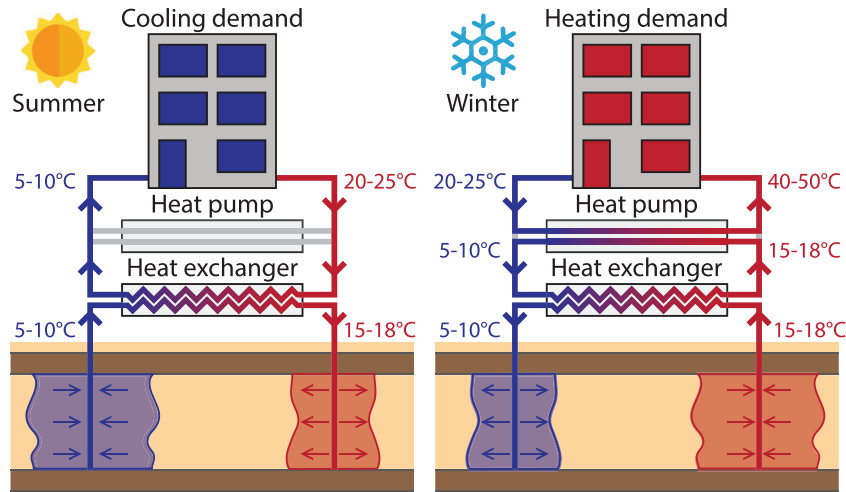


**Figure 1. Basic working principle of an ATEs system.**

exhibit safety margins between wells to prevent a decrease in efficiency due to the adverse interaction between wells (e.g., NVOE 2006). These guidelines protect the interest of existing systems and can lead to significant unused aquifer space between wells. As a result, the current guidelines do not lead to an optimal use of the available aquifer space and limits the number of ATEs systems in a certain area.

Alternative planning approaches have been studied to utilize more subsurface space for thermal energy storage while safeguarding individual system performance. The basic principle is that the loss of thermal energy to the aquifer is reduced when the warm water (or cold water) zones of ATEs systems overlap each other. For example, Bakr et al. (2015) found a performance increase of 1% to 20% due to the positive effects of interaction between wells of the same temperature. Sommer et al. (2014) focused on maximizing the energy stored by ATEs, and found that the largest amount of energy can be stored when wells with the same storage volume are placed in lanes of cold and warm wells (and in line with the groundwater flow direction, if the background flow is significant); they found that the optimal distance between lanes is 2.8 and 3.3 times the thermal radius, and the optimal distance between wells in a lane is 0.41 and 0.56 times the thermal radius. Bloemendal et al. (2018) proposed self-organization of well locations with general design rules until 25% of the aquifer is used for storage; optimal distances between wells of the same temperature and between wells of opposite temperature were determined based on individual system efficiency and reduction of energy to run the system. However, the cited studies did not quantify the effect of the interaction between wells, which includes the assessment of the change in required pumping energy resulting from close well placement.

The objective of this paper is to quantify the increase and decrease in performance when two ATEs systems are placed close together. This is done by taking into account whether an increase in efficiency outweighs an increase in required pumping energy. Insights in the

trade-off between an increase in thermal performance and a simultaneous increase in required pumping energy are needed for optimal utilization of the subsurface for ATEs in order to facilitate the energy transition.

In this paper, the interaction of two ATEs systems is simulated with a numerical model. ATEs systems of different sizes and under different geohydrologic conditions are considered. This paper is organized as follows. First, the basic concepts of ATEs systems are reviewed briefly. Next, the setup of three sets of numerical experiments is described, followed by the assessment framework, the modeling approach, and the results. The paper ends with discussion and conclusions.

## ATEs Systems

ATEs systems inject thermal energy into the aquifer. Part of the injected energy is lost to the surroundings due to conduction, dispersion, and diffusion and cannot be recovered. Conduction losses generally dominate dispersion losses in ATEs systems (e.g., Bloemendal and Hartog 2018).

As an example, consider the simplified case of a fully penetrating well that injects warm water into a homogeneous aquifer with a horizontal, impermeable, and isolating top and bottom; the aquifer thickness is  $H$ . Dispersion and heat conduction are neglected and the aquifer and water are approximated to be at instantaneous thermal equilibrium. For such a case, the injected water forms a cylinder with radius  $R_h$  and height  $L$  equal to the screen length, so that  $R_h$  is equal to

$$R_h = \sqrt{\frac{V}{n\pi L}} \quad (1)$$

where  $V$  ( $\text{m}^3$ ) is the injected volume, and  $n$  is the porosity of the aquifer. The radius  $R_h$  is called the hydraulic radius (Figure 2). Note that the well is fully penetrating so that  $L$  is equal to the aquifer thickness  $H$ . The aquifer volume in thermal equilibrium with the injected water is

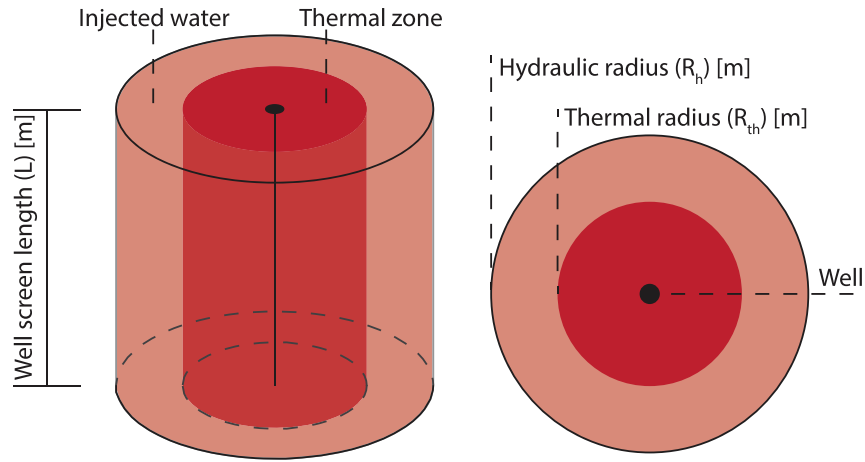


**Figure 2.** Cylinder representing the zone of injected water: the hydraulic radius ( $R_h$ , shaded pink) and the thermal zone: the thermal radius ( $R_{th}$ , red) measured in radial direction from a well.

called the thermal zone and is smaller than the zone of injected water because energy is used to warm up the soil particles. The radius of the thermal zone is called the thermal radius  $R_{th}$  (Figure 2). The thermal radius is computed as

$$R_{th} = \sqrt{\frac{c_w V}{c_a \pi L}} \quad (2)$$

where  $c_w$  (J/m<sup>3</sup>/K) is the volumetric heat capacity of water, and  $c_a$  (J/m<sup>3</sup>/K) is the volumetric heat capacity of the saturated aquifer. The ratio of the well screen length over the thermal radius ( $L/R_{th}$ ) determines the cylindrical shape of the thermal zone. A small  $L/R_{th}$  ratio means that the thermal radius is large compared to the length of the well screen so that the cylinder is short and wide. In practice,  $L/R_{th}$  ratios vary roughly between 0.25 and 4 (e.g., Bloemendal and Hartog 2018).

Energy losses occur mainly at the boundary of the thermal zone. Minimization of the area  $A$  of the thermal zone compared to the volume  $V$  of the thermal zone leads to lower losses (e.g., Bloemendal and Hartog 2018). The lowest  $A/V$  ratios and highest efficiencies are obtained for systems with a large storage volume and an  $L/R_{th}$  ratio of 2 (e.g., Bloemendal and Hartog 2018). For example, Doughty et al. (1982) found that losses to the surrounding aquifer are relatively large compared to losses to the confining layers at the top and bottom of an aquifer, leading to an optimal value of the  $L/R_{th}$  ratio of 1.5.

Energy losses are highest in the first cycle and decrease with consecutive cycles because the temperature of the aquifer near the well adjusts to the temperature of the injected water in the first cycles (e.g., Doughty et al. 1982). The efficiency remains relatively constant after several cycles. The efficiency of ATEs systems commonly ranges from 70% to 90% (e.g., Gao et al. 2017).

## Methods

The assessment of the interaction between multiple ATEs wells is carried out in a simulation study. Three sets

of numerical experiments are conducted. First, the positive effect of combining two ATEs systems into one ATEs system is assessed, which results in the maximum thermal performance increase. Second, the effect of varying the distance between two ATEs systems is investigated, as combining two ATEs systems into one ATEs system is practically seldom possible. Third, the negative effect of an increase in pumping energy is assessed when two ATEs systems are close to each other.

## Setup and Experiments

For all experiments, two ATEs systems are considered (Figure 3). The distance between the two wells with opposite temperature of one ATEs system is  $D_o$  times the thermal radius  $R_{th}$ . The distance between two wells from different ATEs systems but with the same temperature is  $D_s$  times the thermal radius.

The ATEs systems are installed in a confined aquifer sandwiched between two 20 m thick clay layers (aquitards). The top of the top clay layer and the bottom of the bottom clay layer are impermeable and insulating. The initial temperature is equal to the ambient groundwater temperature of 12 °C everywhere. The injection temperature is 7 °C for the cold well and 17 °C for the warm well.

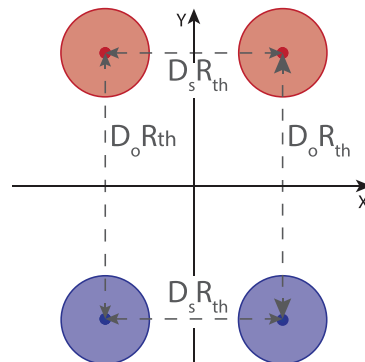


**Figure 3.** Layout of two ATEs systems used for the simulations.

**Table 1**  
Parameter Values or Parameter Ranges Used in the Experiments

Parameter	Experiment 1	Experiments 2 and 3
$V$ (m <sup>3</sup> )	0 to 350,000	250,000 and 50,000
$L/R_{th}$	0.25 to 4	1.35
$D_o$	N/A	2 to 5
$D_s$	0 and $\infty$	0 to 3

**Table 2**  
Hydraulic and Thermal Properties of the Aquifer and Clay Layer

Parameter	Symbol	Value	Units
Porosity	$n$	0.3	—
Horizontal hydraulic conductivity aquifer	$k_{h,s}$	35	m/d
Vertical hydraulic conductivity aquifer	$k_{v,s}$	7	m/d
Horizontal hydraulic conductivity aquitard	$k_{h,c}$	0.05	m/d
Vertical hydraulic conductivity aquitard	$k_{v,c}$	0.01	m/d
Density sand and clay material	$\rho_{s/c}$	2640	kg/m <sup>3</sup>
Density water	$\rho_w$	1000	kg/m <sup>3</sup>
Thermal conductivity aquifer material	$\kappa_s$	3	J/s/m <sup>2</sup> °C
Thermal conductivity aquitard material	$\kappa_c$	1	J/s/m <sup>2</sup> °C
Thermal conductivity water	$\kappa_w$	0.58	J/s/m <sup>2</sup> °C
Specific heat capacity sand and clay material	$c_{p,s/c}$	0.71	kJ/kg°C
Specific heat capacity water	$c_{p,w}$	4.18	kJ/kg°C

Different representative storage volumes  $V$  are considered (Table 1), but the applied injection/extraction is always the same for both ATES systems. The discharge  $Q$  of the wells is based on  $V$ , and is distributed over the year using a sine function.

The hydraulic properties of the aquifer and aquitards are summarized in Table 2, which also includes the thermal properties of the aquifer material (sand) and aquitard material (clay). The bulk values of the density, thermal conductivity, and heat capacity are obtained as the volume-weighted average of the properties of the solid and water fractions. For example, the bulk density  $\rho_b$  is computed from the density of the water  $\rho_w$  and the density of the sand  $\rho_s$  as

$$\rho_b = n\rho_w + (1 - n)\rho_s \quad (3)$$

where  $n$  is the porosity.

#### Experiment 1: Maximum Positive Effect of Combining Two ATES Systems

The objective of the first experiment is to determine the maximum thermal performance of two ATES systems.

The maximum thermal performance is obtained when the two ATES systems are combined (i.e.,  $D_s = 0$ ) and the distance between the warm and the cold well ( $D_o$ ) is so large that the warm well does not effect the performance of the cold well and vice versa. The thermal performance of the combined ATES systems is compared to the thermal performance of a single ATES system.

The improvement in thermal recovery efficiency is calculated for systems with different shapes and storage volumes, as summarized in Table 1. The  $L/R_{th}$  ratio determines the shape of the storage volume and is varied between 0.25 and 4. The storage volume is varied between 0 and 350,000 m<sup>3</sup>/year, which are common values for ATES systems in the Netherlands (e.g., Bloemendal and Hartog 2018). The aquifer thickness (in this case equal to the well screen length) used in the simulation follows from the specified storage volume  $V$  and  $L/R_{th}$  ratio simulated, using Equation 2. The area over volume ratio ( $A/V$ ) is computed for the combined system and for a single system.

#### Experiment 2: Positive and Negative Interaction Between Two ATES Systems

The objective of the second experiment is to determine the change in thermal performance when the distance between the two ATES systems  $D_s R_{th}$  and the distance between wells of opposite temperature  $D_o R_{th}$  vary. The distances are varied as specified in Table 1 and the thermal recovery efficiency is calculated. The change in recovery efficiency is determined by comparing the recovery efficiency of each ATES system with the maximum increase that can be obtained by combining two ATES systems.

Two average-sized systems (for Dutch market conditions) with the same storage volume of 250,000 m<sup>3</sup> and the same  $L/R_{th}$  ratio of 1.35 are placed in a rectangular configuration (Figure 3). The distances between wells of the same temperature ( $D_s R_{th}$ ) and the distances between wells of opposite temperature ( $D_o R_{th}$ ) are varied. The same approach is repeated for two smaller systems with a storage volume of 50,000 m<sup>3</sup>, which is sufficient to provide thermal energy for small buildings.

#### Experiment 3: Trade-off Between Increase in Thermal Efficiency and Pumping Energy

The drawdown in each well is calculated for the maximum well discharge in Experiment 2. The increase in the drawdown is compared with the drawdown for each well in a simulation with no hydraulic interactions between the wells ( $D_o = D_s = \infty$ ). The increase in drawdown is translated to an increase in required pumping energy for running the ATES system. It is assumed that an increase in drawdown is linearly related to an increase in pumping energy. The trade-off between an increase in thermal recovery efficiency and an increase in pumping energy is assessed.

#### Assessment Framework

The performance of ATES systems is quantified by the thermal recovery efficiency (Doughty et al. 1982;

Bloemendal and Hartog 2018) and the pumping energy. The thermal recovery efficiency  $\eta_{th}$  is defined as the extracted thermal energy in one extraction period as a percentage of the injected thermal energy in the previous injection period and is calculated for every cycle as:

$$\eta_{th} = \frac{E_{ex}}{E_{in}} = \frac{\int_0^t Q_{ex} c_w \Delta T dt}{\int_0^t Q_{in} c_w \Delta T dt} \quad (4)$$

where  $E_{ex}$  and  $E_{in}$  (J) are the extracted and injected energy, respectively,  $Q_{ex}$  and  $Q_{in}$  (m<sup>3</sup>/d) are the well discharge during extraction and injection, respectively,  $\Delta T$  (°C) is the absolute temperature difference between the injected or extracted water and the background temperature of the aquifer,  $c_w$  is the volumetric heat capacity of the groundwater, and  $t$  (d) is time.

The effect of other wells on the thermal performance of one well is expressed as the relative change of the efficiency using the approach of for example, Bakr et al. (2015). First, the thermal recovery efficiency of one well is computed, in absence of other wells ( $\eta_{one}$ ). Next, the thermal recovery efficiency of the same well is computed, but now with the other wells in operation ( $\eta_{all}$ ). The change in recovery efficiency due to the presence of the other wells is expressed as the relative change in efficiency ( $\varepsilon$ , -).

$$\varepsilon = \frac{\eta_{all} - \eta_{one}}{\eta_{one}} \quad (5)$$

The pumping energy depends on the drawdown in the pumping well, the injection pressure in the injection well, and the losses in the pipes. The drawdown  $d$  in the pumping well is estimated from a steady-state solution as:

$$d = -\frac{Q}{2\pi k_{h,s} H} \ln \left( \frac{r_w D_s}{D_o R_{th} \sqrt{D_o^2 + D_s^2}} \right) \quad (6)$$

where  $r_w$  (m) is the radius of the well (set to 0.3 m here). The total hydraulic head  $h_p$  that the pump of an ATEs system (extraction and an injection well) needs to overcome is:

$$h_p = h_s + 2|d| \quad (7)$$

where  $h_s$  (m) is the head loss in the pipe system approximated as 20 m; possible changes in the head loss due to expansion of the pipe systems are neglected. The required pumping energy  $E_p$  (J) is calculated from the hydraulic head loss as:

$$E_p = \int_0^t Q \rho_w g h_p dt \quad (8)$$

where  $g$  (m/s<sup>2</sup>) is the acceleration of gravity.

The advantage of an increase in thermal recovery efficiency must outweigh any increase in pumping energy.

The coefficient of performance  $COP$  (-) is used to assess the overall performance of the system.

$$COP = \frac{E_{ex}}{E_p} \quad (9)$$

The relative change in  $COP$  ( $\gamma$ , -) due to the presence of other wells is calculated similarly to Equation 5 as:

$$\gamma = \frac{COP_{all} - COP_{one}}{COP_{one}} \quad (10)$$

## Modeling Approach

Combined groundwater flow and heat transport is modeled with SEAWAT. SEAWAT (version 4) combines MODFLOW (version 1.18.01) and MT3DMS (version 5.20). Python is used as an interface to construct input files and to process SEAWAT output using the floppy package (e.g., Bakker et al. 2016). SEAWAT is designed to simulate three-dimensional, variable density groundwater flow and multi-species transport (e.g., Langevin et al. 2008). Heat transport is simulated by treating heat as one of the solute species following, for example, Thorne et al. (2006). This is possible due to the similarity in the mathematical description of solute transport (Fick's law) and heat transport (Fourier's law). To account for thermal retardation, the first order sorption coefficient in MT3DMS is replaced by the thermal distribution factor ( $K_{d,temp}$ ) defined as (e.g., Langevin et al. 2008):

$$K_{d,temp} = \frac{c_{p,s/c}}{\rho_w c_{p,w}} \quad (11)$$

Application of the values in Table 2 results in  $K_{d,temp} = 1.7 \times 10^{-4}$  m<sup>2</sup>/kg. The molecular diffusion coefficient ( $D_m$ ) in MT3D is replaced by the thermal diffusion ( $D_{m,temp}$ ) as (e.g., Langevin et al. 2008):

$$D_{m,temp} = \frac{\kappa_b}{n \rho_w c_{p,w}} \quad (12)$$

where  $\kappa_b$  is the bulk thermal conductivity of the subsurface material. Application of the values in Table 2 results in  $D_{m,temp} = 0.15$  m<sup>2</sup>/d. The longitudinal dispersivity is 0.5 m, and the transverse and vertical dispersivity are both one tenth of the longitudinal dispersivity.

Following the experimental setup illustrated in Figure 3, a rectangular model area is used of 2400 by 2400 m. A constant head and temperature boundary are used at the lateral edges of the model area. The ATEs wells are placed in the center area of 400 by 400 m, in which the grid cells are 4 by 4 m. Beyond this center-area, the grid cells expand to 150 by 150 m at the boundary of the model, Figure 4. The height of the grid cells is 5 m everywhere. Exploratory simulations were conducted with varying cell sizes and model extent, which showed that smaller cell sizes and a larger model area did not change the results significantly.

Each experiment is run for 5 years (5 cycles) with a time step for MODFLOW of 30 d. The Courant condition

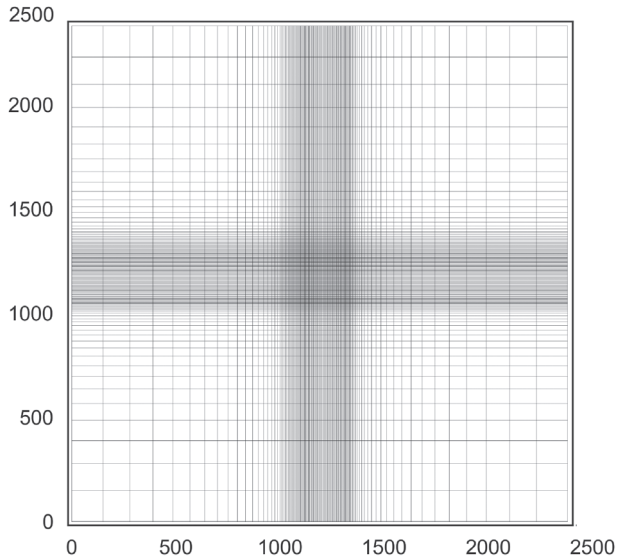


Figure 4. Schematic representation of the grid.

is set to 0.8 in MT3DMS; MT3DMS automatically reduces the time step to meet this condition. After 5 cycles, the recovery efficiency is approximately 90% of the recovery efficiency, that is, eventually reached after many cycles (e.g., Bakr et al. 2015). The preconditioned conjugate gradient (PCG) method is used to solve for the flow field. The finite difference method is used to solve for the heat transport. The aquifer and flow are approximated as incompressible, so that the flow of groundwater can be simulated as instantaneous steady state. The effect of relatively small temperature changes on the viscosity and density are neglected (Doughty et al. 1982; Bloemendal and Hartog 2018).

## Results

### Experiment 1: Maximum Positive Effect of Combining Two ATES Systems

The thermal recovery efficiency  $\eta_{th}$  (Equation 4) of an ATES well after 5 cycles is plotted as a function of the storage volume in Figure 5 for different values of  $L/R_{th}$ . As expected, the thermal recovery efficiency is higher for larger storage volumes and smaller values of  $L/R_{th}$ . The recovery efficiency is in the range 35% to 45% for a relatively small system ( $V = 50,000 \text{ m}^3$ ) and in the range 50% to 60% for larger system ( $V = 250,000 \text{ m}^3$ ).

The maximum increase in thermal recovery efficiency of two ATES systems with the same storage volume is obtained when the two ATES systems are combined into one ATES systems. This is equivalent to doubling the storage volume of the ATES system. The relative increase in thermal recovery efficiency  $\varepsilon$  (Equation 5) by combining two ATES systems with the same storage volume is plotted in Figure 6. Systems with a small storage volume and/or a larger  $L/R_{th}$  value have a larger relative increase in thermal recovery efficiency when they are combined. The relative increase is in the range

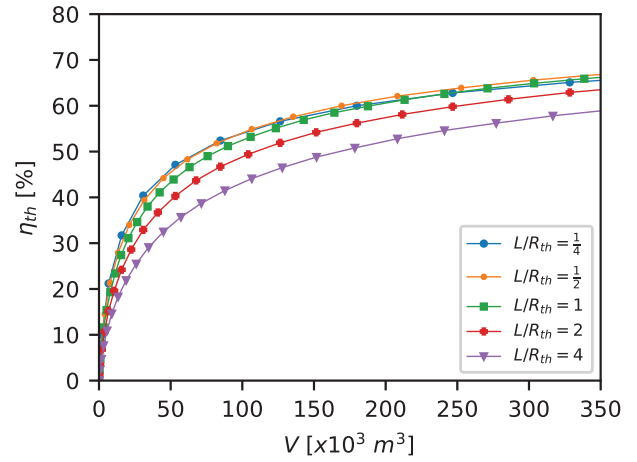


Figure 5. Thermal recovery efficiency ( $\eta_{th}$ ) of an ATES well after 5 cycles for different storage volumes ( $V$ ) and storage shapes ( $L/R_{th}$ ).

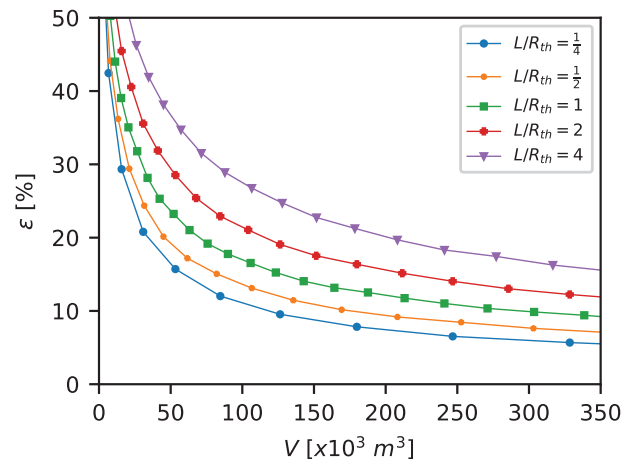
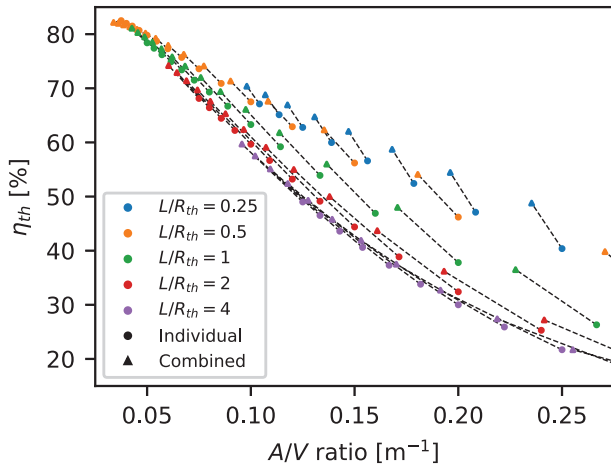


Figure 6. Maximum relative increase in thermal recovery efficiency  $\varepsilon$  by combining two ATES wells of the same temperature after 5 cycles for different storage volumes ( $V$ ) and storage shapes ( $L/R_{th}$ ).

15% to 35% for a relatively small system ( $V = 50,000 \text{ m}^3$ ) and in the range 10% to 20% for a larger system ( $V = 250,000 \text{ m}^3$ ).

The thermal recovery efficiency is plotted versus the area over volume ratio ( $A/V$ ) for two individual systems (circles) and one combined system (triangles) (Figure 7); the dashed black lines connect the value of the two individual systems with the corresponding combined system. The combined systems have a smaller  $A/V$  ratio and a larger recovery efficiency than the two individual systems. Individual systems with a large  $A/V$  ratio (relatively small systems with long well screens) have the largest decrease in the  $A/V$  ratio when two systems are combined, leading to the largest increase in efficiency. The relation between a smaller recovery efficiency and a larger  $A/V$  ratio was previously reported by Bloemendal and Hartog (2018). Systems with a relatively large thermal radius (small  $L/R_{th}$  ratio) have a higher efficiency for the same  $A/V$  ratio. This is



**Figure 7. Thermal recovery efficiency ( $\eta_{th}$ ) vs.  $A/V$  ratio for different storage volumes ( $V$ ) and storage shapes ( $L/R_{th}$ ). The dashed lines show the decrease in  $A/V$  and increase in efficiency when two systems are combined.**

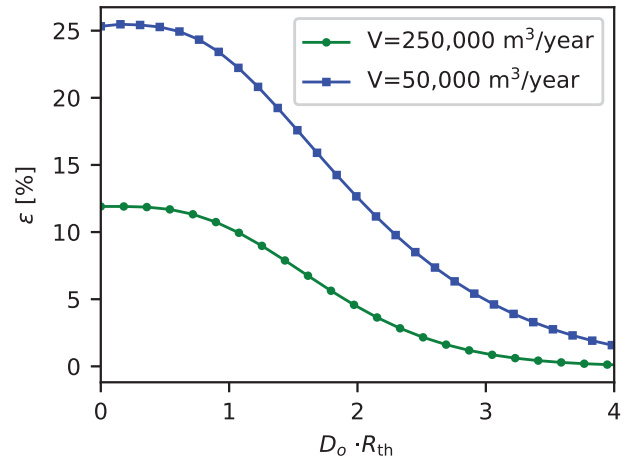


**Figure 9. Relative change in recovery efficiency ( $\varepsilon$ ) as a function of the distance  $D_s$  between two wells of the same temperature for two storage volumes and storage shape  $L/R_{th} = 1.35$ .**

likely because conduction losses to the aquifer are large compared to the losses to the confining layers (e.g., Doughty et al. 1982).

### Experiment 2: Positive and Negative Interaction Between Two ATES Systems

The interaction between two ATES systems is illustrated in Figure 8. The temperature distribution at the end of the summer injection period of the fifth cycle is shown for two ATES systems. The temperature distribution for two systems that are relatively far apart is shown in Figure 8a; the interaction between the systems is negligible. The temperature distribution when wells with the same temperature are placed close together is shown in Figure 8b. The thermal zones are combined, which leads to an increase in performance. The temperature distribution when wells with the opposite temperature are also placed close together is shown in Figure 8c. Now the warm water has actually reached the cold well. The

cold well is extracting warm water and the performance decreases.

The thermal recovery efficiency of two ATES systems increases when the wells of the same temperature are placed closer together ( $D_s$  is small as in Figure 8a). The increase in thermal recovery efficiency  $\varepsilon$  is plotted vs.  $D_s$  in Figure 9 for both a small and a large system. For this simulation,  $D_o$  is chosen large, so that there is a negligible effect of the wells of opposite temperature on the thermal recovery efficiency. The relative increase in recovery efficiency is larger for the smaller system. The maximum relative increase is approximately 25% for the small system and approximately 12% for the large system. The increase in recovery efficiency is relatively constant for  $D_s$  between 0 and 1, and decreases for  $D_s > 1$ .

The change in thermal recovery efficiency as a function of both the distance between wells of the same temperature ( $D_s$ ) and the distance between wells of opposite temperature ( $D_o$ ) is shown in Figure 10

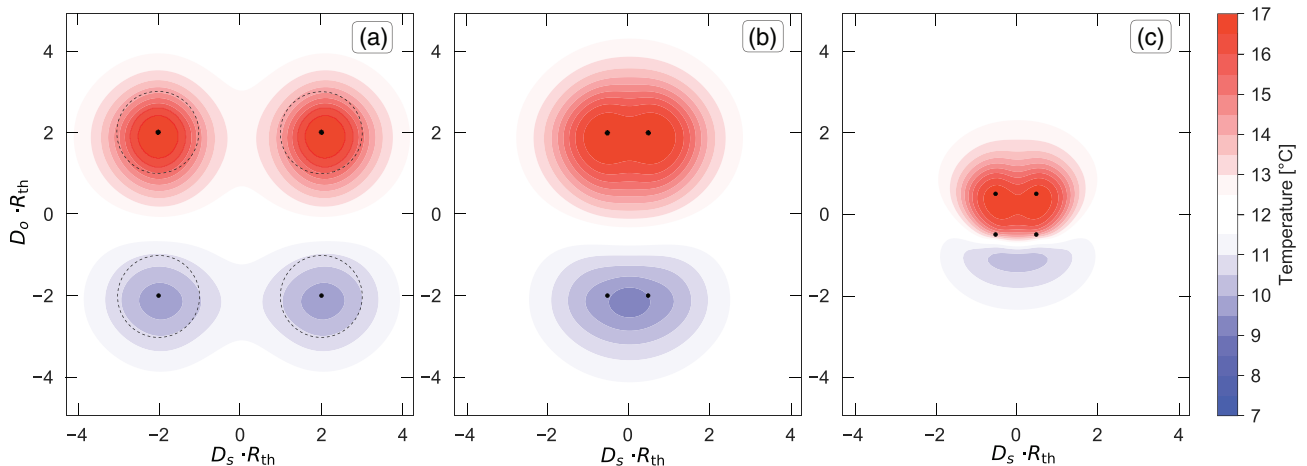


**Figure 8. Temperature distribution for different well distances at the end of summer. (a)  $D_o = D_s = 4$ , (b)  $D_o = 4, D_s = 1$  (c)  $D_o = D_s = 1$ . The dotted lines in (a) indicate the thermal radius  $R_{th}$  from Equation 2.**

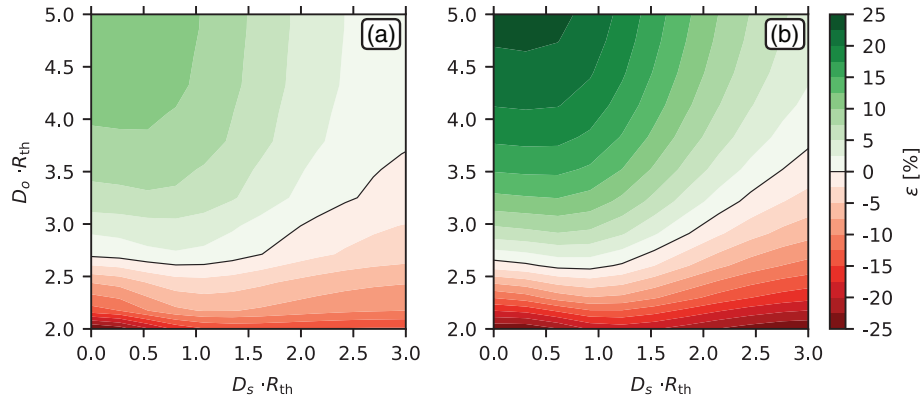


**Figure 10.** Relative change in thermal recovery efficiency ( $\epsilon$ ) as a function of the distance  $D_o$  between wells of opposite temperature and the distance  $D_s$  of wells with the same temperature for storage volumes of 250,000 m<sup>3</sup> (a) and 50,000 m<sup>3</sup> (b) and an  $L/R_{th}$  ratio of 1.35. The top rows in the subplots are also shown in Figure 9.

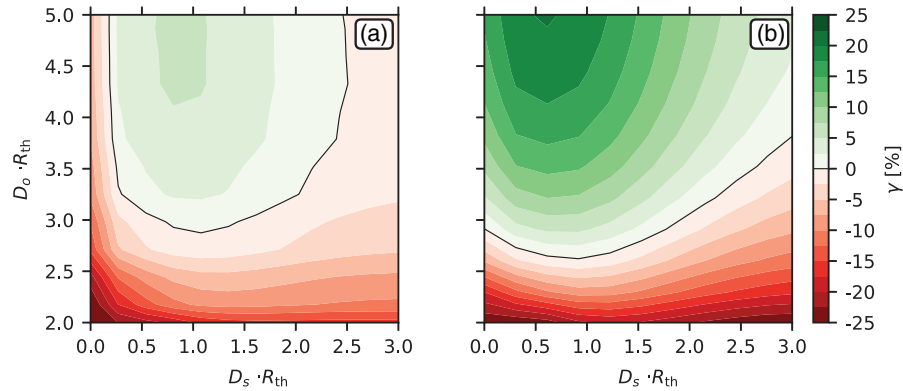


**Figure 11.** The relative change  $\gamma$  in coefficient of performance ( $COP$ ) when two ATEs systems are close together for a storage volume of 250,000 m<sup>3</sup>/year (a) and 50,000 m<sup>3</sup>/year (b) and  $L/R_{th} = 1.35$ .

for a small and a large system. A minimum distance between wells of opposite temperature is needed to avoid a decrease in efficiency. The black contour in Figure 10 represents configurations that do not lead to a change in the recovery efficiency of the combined system. The efficiency of the combined system increases when the distance between wells of opposite temperature is larger than approximately 2.6 times the thermal radius. The negative effect of wells of opposite temperature can be neglected when the distance between wells of opposite temperature is larger than 4.5 times the thermal radius. When  $D_o > 4.5$ , the change in thermal recovery efficiency depends only on the distance between wells of the same temperature, resulting in the graph of Figure 9.

### Experiment 3: Trade-off Between Increase in Thermal Efficiency and Pumping Energy

The advantage of an increase in thermal recovery efficiency must outweigh the increase in pumping energy due to the increase in drawdown in the well. The combined effect of the increase in thermal recovery efficiency and the increase in pumping energy, expressed as the change  $\gamma$  (Equation 10) of the coefficient of performance ( $COP$ ), is shown in Figure 11 for both a larger system and a smaller system. For the larger system

(Figure 11a), the negative effect of increased pumping energy outweighs the positive effects of the increased thermal recovery efficiency when the distance between wells of the same temperature is small. The combined effect is positive when a small distance between wells of the same temperature is applied because the change in drawdown decreases exponentially while the change in thermal recovery efficiency can be approximated as constant between 0 and 1  $R_{th}$ . Therefore, a distance of 0.5 times the thermal radius is sufficient to improve overall system performance, while the optimum is around 1  $R_{th}$ . For the smaller system (Figure 11b), the relative increase in  $COP$  is positive also for  $D_s = 0$ , as long as  $D_o > 3$ . The maximum relative increase in  $COP$  is much larger for the smaller system than for the larger system.

### Discussion

The objective of ATEs application is to reduce primary energy use by the facilities in the buildings (e.g., heat pump, circulation pumps, peak supply) and depends on the mode of operation of the ATEs system. To what extent improved recovery efficiency of the wells affect primary energy use depends on the mode of operation of the ATEs system.



- In the case of cooling, the primary energy use is expected to decrease with a higher rate than the increase in thermal recovery efficiency of the groundwater system of the ATEs. Because in summer cooling is provided directly without the use of a heat pump or cooling machine. Increased recovery efficiency means that cold water can be extracted for a longer period. Resulting that the use of the heat pump for cooling at the end of the summer can be reduced or is avoided entirely, which constitutes a significant energy savings as the required primary energy use for cooling from ATEs and with heat pump differs by a factor of about 10 (e.g., Bloemendal et al. 2018).
- In the case of heating, the primary energy use is expected to decrease with a lower rate than the increase in thermal recovery efficiency of the groundwater system. In any case a heat pump is needed to provide heating in the winter. A higher efficiency of the warm well leads to a higher average temperature at the evaporator of the heat pump. This means that the energy consumption of the heat pump is reduced, but with a lower rate than the increase of the thermal recovery efficiency. This is caused by the fact that the efficiency of the heat pump depends on the Carnot cycle, which is based on absolute temperatures (Kelvin scale) (Carnot 1978).

Overall, the improved recovery efficiency due to combination of thermal zone of well is expected to result in limited primary energy use reduction. At the same time, reduction of mutual distance between wells allows accommodation of more ATEs wells, which in turn allows better utilization of subsurface space and gives access to ATEs technology for more buildings. Various studies (e.g., Sommer et al. 2015; Bloemendal et al. 2018) showed that high adoption rates of ATEs have a significant impact on the primary energy use savings for buildings in an area.

The presented advantage of combining the thermal zones of two ATEs systems is based on an idealized situation. Confirmation of our findings with an experiment in the field is difficult, as it would require data of multiple years of operation of a single ATEs system, followed by data for multiple years of the same ATEs system, but now with a nearby ATEs system in operation. As such an experiment is hardly feasible. The most important idealizations of the followed approach in this study and their effects on the outcomes of this study are discussed below.

- Wells are placed on the corners of a rectangle. The performance of a nonrectangular layout will likely be similar to the performance of a rectangular layout provided that the area over volume ratio ( $A/V$ ) of the combined system decreases in a similar manner as for the rectangular layout.
- The injection temperatures of the two systems are the same. The increase in performance may decrease when the injection temperatures are different. For example, if one system injects warm water at  $16^{\circ}\text{C}$  and the other system at  $18^{\circ}\text{C}$ , then the increase in performance of

the warmer system will be smaller than the increase in performance of the colder system.

- The systems are balanced. In practice, the balance between the warm and cold well will vary over time due to variations in outside air temperature and energy use by the buildings over the years. A combined system may benefit when two systems have an opposite imbalance as, for example, the excess warm water of one system may be used by the other system. Systems with a structural imbalance (e.g., systems that always extract more energy for cooling than for heating) will negatively effect the performance of a nearby system, as the imbalanced system will extract an unequal share of the energy injected by the other system.
- Systems may pump significantly less than the permitted amount, which is used to design the system. The increase in performance by combining ATEs systems must be determined for the actual storage volume.
- More than two ATEs systems may be combined. The thermal recovery efficiency is expected to increase when more than two ATEs systems are placed close together, provided that the  $A/V$  ratio of the combined system is smaller than for the uncombined systems. The relative increase will likely be smaller for every subsequent system, that is, added.
- ATEs is simulated in homogeneous aquifers with no background flow. The effect of heterogeneity and background flow on the performance of ATEs systems has been addressed in various studies (e.g., Sommer et al. 2013; Bloemendal and Hartog 2018; Bloemendal and Olsthoorn 2018). Heterogeneity may impact recovery efficiency when heterogeneity is significant (e.g., when thin gravel layers are present) and wells of opposite type are placed close together. However, average heterogeneous condition do not affect recovery considerably. Hence, from these previous studies it is concluded that heterogeneity will not affect the outcomes and conclusions of this study. Low groundwater flow velocities ( $<25\text{ m/year}$ ) generally have limited impact on ATEs recovery efficiency. The effect of background flow must be taken into account for ATEs well placement at flow rates above  $25\text{ m/year}$  (Bloemendal and Hartog 2018; Bloemendal and Olsthoorn 2018). Clustering of wells of the same type reduces the effect of background flow. Wells of the opposite type should, of course, not be placed in line with the background flow. In high groundwater flow aquifers densely occupied with ATEs systems, lanes of warm and cold wells should be made in line with the groundwater flow direction.

## Conclusion

The performance of two ATEs systems increases when their thermal zones are combined. Losses of thermal energy occur at the boundaries of the thermal zones. The efficiency of individual ATEs systems increases when wells of the same temperature are placed close together, because the  $A/V$  ratio, the area of the thermal zone

relative to the volumes, is reduced. The combination of two smaller systems (storage volume of 50,000 m<sup>3</sup>) results in an increase in thermal energy efficiency up to 25% for the systems considered. The combination of two larger systems (storage volume of 250,000 m<sup>3</sup>) results in a smaller increase in thermal energy efficiency of up to 12%. The increase of thermal recovery efficiency depends on the shape of the thermal zone, expressed by ratio of the fully penetrating well screen  $L$  over the thermal radius  $R_{th}$ . Combination of ATES systems with a relatively long well screen (large  $L/R_{th}$  ratio) results in a higher increase of the thermal recovery efficiency than combination of systems with a relatively short well screen (low  $L/R_{th}$  ratio).

The combination of two ATES systems may lead to an increase in thermal recovery efficiency, but it also results in an increase in required pumping energy. An increase of the total system performance, expressed as the coefficient of performance, is obtained when wells of the same temperature are placed approximately  $0.5R_{th}$  apart. The distance between wells of opposite temperature must be larger than  $3R_{th}$  to avoid a decrease in efficiency due to interaction between the warm and cold wells. In practice, the optimal distance between wells of opposite temperature should be chosen based the trade-off between an increase in individual system performance and optimal use of the available aquifer space.

## Acknowledgments

The authors thank Jannis Epting, one anonymous reviewer and the editor for their feedback and suggestions for improvements. Furthermore we thank Anne Medema for his insights and input on the research.

## Authors' Note

The authors do not have any conflicts of interest or financial disclosures to report.

## References

- Bakker, M., V. Post, C.D. Langevin, J.D. Hughes, J.T. White, J.J. Starn, and M.N. Fioren. 2016. Scripting MODFLOW model development using python and FloPy. *Groundwater* 54, no. 5: 733–739. <https://doi.org/10.1111/gwat.12413>
- Bakr, M., N. van Oostrom, and W. Sommer. 2015. Efficiency of and interference among multiple aquifer thermal energy storage systems; a Dutch case study. *Renewable Energy* 60: 53–62. <https://doi.org/10.1016/j.renene.2013.04.004>
- Bloemendal, M., and N. Hartog. 2018. Analysis of the impact of storage conditions on the thermal recovery efficiency of low-temperature ATES systems. *Geothermics* 71: 306–319. <https://doi.org/10.1016/j.geothermics.2017.10.009>
- Bloemendal, M., and T.N. Olsthoorn. 2018. ATES systems in aquifers with high ambient groundwater flow velocity. *Geothermics* 75: 81–92. <https://doi.org/10.1016/j.geothermics.2018.04.005>
- Bloemendal, M., M. Jaxa-Rozen, and T.N. Olsthoorn. 2018. Methods for planning of ATES systems. *Applied Energy* 216: 534–557. <https://doi.org/10.1016/j.apenergy.2018.02.068>
- Bloemendal, M., T. Olsthoorn, and F. van de Ven. 2015. Combining climatic and geo-hydrological preconditions as a method to determine world potential for aquifer thermal energy storage. *Science of the Total Environment* 538, no. 2015: 621–633. <https://doi.org/10.1016/j.scitotenv.2015.07.084>
- Carnot, S. 1978. *Réflexions sur la puissance motrice du feu*. Paris: Librairie Scientifique et Technique.
- Doughty, C., G. Hellström, and C.F. Tsang. 1982. A dimensionless parameter approach to the thermal behaviour of an aquifer thermal energy storage system. *Water Resources Research* 18, no. 3: 571–587. <https://doi.org/10.1029/WR018i003p00571>
- Gao, L., J. Zhao, Q. An, and J., Wang, and Liu, X. 2017. A review on system performance studies of aquifer thermal energy storage. *Energy Procedia* 142: 3537–3545. <https://doi.org/10.1016/j.egypro.2017.12.242>
- Langevin, C. D., D. T. Thorne, A. M. Dausman, M. C. Sukop, and W. Guo. 2008. SEAWAT Version 4: A computer program for simulation of multi-species solute and heat transport. U.S. Geological Survey Techniques and Methods, Book 6, Chapter A22, 39 p. Reston, Virginia: USGS.
- NVOE (Dutch association for Underground thermal energy storage). 2006. Methods and guidelines for underground energy storage (in Dutch).
- REN21. 2017. Renewables 2017 global status report. Paris. Available at: [http://www.ren21.net/gsr\\_2017\\_full\\_report\\_en](http://www.ren21.net/gsr_2017_full_report_en)
- Sommer, W., J. Valstar, I. Leusbrock, T. Grotenhuis, and H. Rijnaarts. 2015. Optimization and spatial pattern of large-scale aquifer thermal energy storage. *Applied Energy* 137: 322–337. <https://doi.org/10.1016/j.apenergy.2014.10.019>
- Sommer, W., J. Valstar, P. van Gaans, T. Grotenhuis, and H. Rijnaarts. 2013. The impact of aquifer heterogeneity on the performance of aquifer thermal energy storage. *Water Resources Research* 49: 8128–8138. <https://doi.org/10.1002/2013wr013677>
- Sommer, W. T., P. J. Doornenbal, B. C. Drijver, P. F. M. van Gaans, I. Leusbrock, J. T. C. Grotenhuis, H. H. M. Rijnaarts. 2014. Thermal performance and heat transport in aquifer thermal energy storage. *Hydrogeology Journal* 22: 263–279.
- Thorne, D., C.D. Langevin, and M.C. Sukop. 2006. Addition of simultaneous heat and solute transport and variable fluid viscosity to SEAWAT. *Computers & Geosciences* 32, no. 10: 1758–1768. <https://doi.org/10.1016/j.cageo.2006.04.005>